

LASER-WELDED V-Cr-Ti ALLOYS: MICROSTRUCTURAL AND MECHANICAL PROPERTIES\*  
K. Natesan, D. L. Smith, P. G. Sanders, and K. H. Leong (Argonne National Laboratory)

OBJECTIVE

The objectives of this task are to (a) determine the optimum parameters for laser beam welding of sheets of V-Cr-Ti alloys; (b) examine the microstructural characteristics of welded sections, including base metal, heat-affected-region, and core of weld; (c) evaluate the influence of different post-welding heat treatments on microstructural characteristics; and (d) evaluate the mechanical properties, such as tensile and impact, of laser-welded materials.

SUMMARY

A systematic study has been initiated to examine the use of lasers to weld sheet materials of V-Cr-Ti alloys and to characterize the microstructural and mechanical properties of the laser-welded materials. In addition, several post-welding heat treatments are being applied to the welded samples to evaluate their benefits, if any, to the structure and properties of the weldments. Hardness measurements are made across the welded regions of different samples to evaluate differences in the characteristics of various weldments.

EXPERIMENTAL PROGRAM

The heat of vanadium alloy selected for the study had a nominal composition of V-4 wt.%Cr-4 wt.%Ti (designated as BL-71). A 4-mm-thick sheet of the alloy was used for the welding study. Seven different welds were made under the same welding conditions but were subsequently given different post-welding heat treatments. Laser beam power was 1325 W and travel speed was 110 mm/s. A lens with a 125 mm focal length was used, and the focus was 1 mm into the material. The beam was 1 mm in diameter and penetration was  $\approx$ 2 mm into the 4-mm-thick sheet.

Shielding gas used was argon with a flow rate of 0.25 L/s, provided by a 9.5-mm-diameter tube at 30° from horizontal. The welds were started and ended on a scrap piece of vanadium so that penetration depth could be seen at both ends of the weld. The vanadium plate was clamped to an aluminum plate, which in turn was clamped to a water-cooled copper block; this arrangement provided sufficient cooling to keep the vanadium sheet barely warm after welding. The heat treatments are listed in Table 1. Weld 3 was in as-welded condition. Welds 1 and 2 were given post-welding heat treatment of 1 and 5 passes, respectively, with a defocused beam 25 mm in diameter. Welds 4 and 5 were post-welding heat treated with  $\approx$ 50% of the power level of welds 1 and 2. Welds 6 and 7 were treated with a power level of 25% of welds 1 and 2. The defocused beams were wider than the welds ( $\approx$ 4 mm beam, compared to 3 mm for the weld).

Table 1. Heat treatments for different laser welds

Weld No.	Beam diameter (mm)	Power (W)	Speed (mm/s)	No. of passes
1	25	1325	1	1
2	25	1325	1	5
3	untreated	-	-	-
4	25	664	0.25	1
5	25	664	0.25	5
6	25	319	0.25	1
7	25	319	0.25	5

Weld cross sections of different specimens were examined by scanning electron microscopy (SEM). In addition, Knoop hardness measurements were made at three different locations in the weld, heat-affected zone, and base metal.

## RESULTS AND DISCUSSION

Figure 1 contains an SEM photomicrograph of the cross section of Weld 3 specimen in the as-welded condition. The weld has a substantial variation in grain size from the root of the weld to the free surface region of the weld. Also, the grains near the top of the weld are columnar, which is dictated by rate of cooling and solidification. Even in the root of the weld, the grains are of the order of two to five times larger than those of the base metal away from the weld. Further, the weld cross section shows definite contours evenly spaced in the root region, along which can occur preferential segregation of impurities. The dark- and light-shaded grains in the weld are due to differences in grain orientation, and virtually no compositional variations were observed between these grains.

In the Weld 3 specimen, Knoop hardness measurements were made at three different elevations and on both sides of the weld centerline. These elevations are designated by A, AA, B, BB, C, and CC, as shown in Figure 1. Knoop hardness profiles at different elevations are also shown in Figure 1 and indicate that the hardness values on either side of the weld centerline were similar at all three elevations examined. The hardness profiles at elevation A and AA indicate a peak value of  $\approx 270$  in the weld zone, while the base metal had values of 165 to 190. At weld elevations B and BB, the weld pool zone had a hardness value of  $\approx 250$  at a depth of 0.35-0.40 mm, beyond which hardness dropped monotonically to base metal values of  $\approx 170$ -190. At elevations C and CC, the hardness profiles indicated a drop in the weld centerline region from 250 to 190-215, while a peak in hardness was noted at a distance of 0.8-0.9 mm from the weld centerline. Since the hardness profile of the weld specimen showed that the profiles are symmetrical on either side of the weld centerline, hardness measurements on subsequent specimens were made on only one side of the weld centerline.

Figure 2 includes an SEM photomicrograph of the cross section of a welded specimen after post-welding heat treatment, designated as Weld 1 in Table 1. As in the as-welded sample, this specimen showed a substantial variation in grain size from the root of the weld to the free surface region. Also, the grains near the top of the weld are columnar, dictated by rate of cooling and solidification. Figure 2 also shows the hardness profiles at elevations A, B, and C in the welded specimen. The effect of one pass of post-welding heat treatment with a defocused laser beam was to soften the material in the weld zone, as indicated by the monotonic decrease in hardness from the weld centerline to the base metal. Even the peak hardness value is somewhat lower and the peak is confined to the region close to the centerline. The impact of such decrease on the mechanical properties of the weld can be substantial and will probably be beneficial.

Figure 3 shows an SEM photomicrograph of the cross section of a welded specimen after post-welding heat treatment, designated as Weld 2 in Table 1. As in the previous samples, this specimen also shows that the weld has a substantial variation in grain size from the root of the weld to the free surface region. Also, the grains near the top of the weld are columnar in shape, again dictated by rate of cooling and solidification. Figure 3 also shows the hardness profiles at elevations A, B, and C in the welded specimen. The effect of five passes of post-welding heat treatment with a defocused laser beam was to soften the material in the weld zone, especially at the root region of weld. The erratic hardness variation in the weld region of this specimen at elevations B and C indicate that grain growth may have occurred in the upper portions of weld as a result of the multiple passes.

Analysis is in progress on additional specimens with the various post-welding heat treatments listed in Table 1. Subsequently, several of these welded specimens will be evaluated for their impact properties in order to establish the role of post-welding heat treatments on mechanical properties.

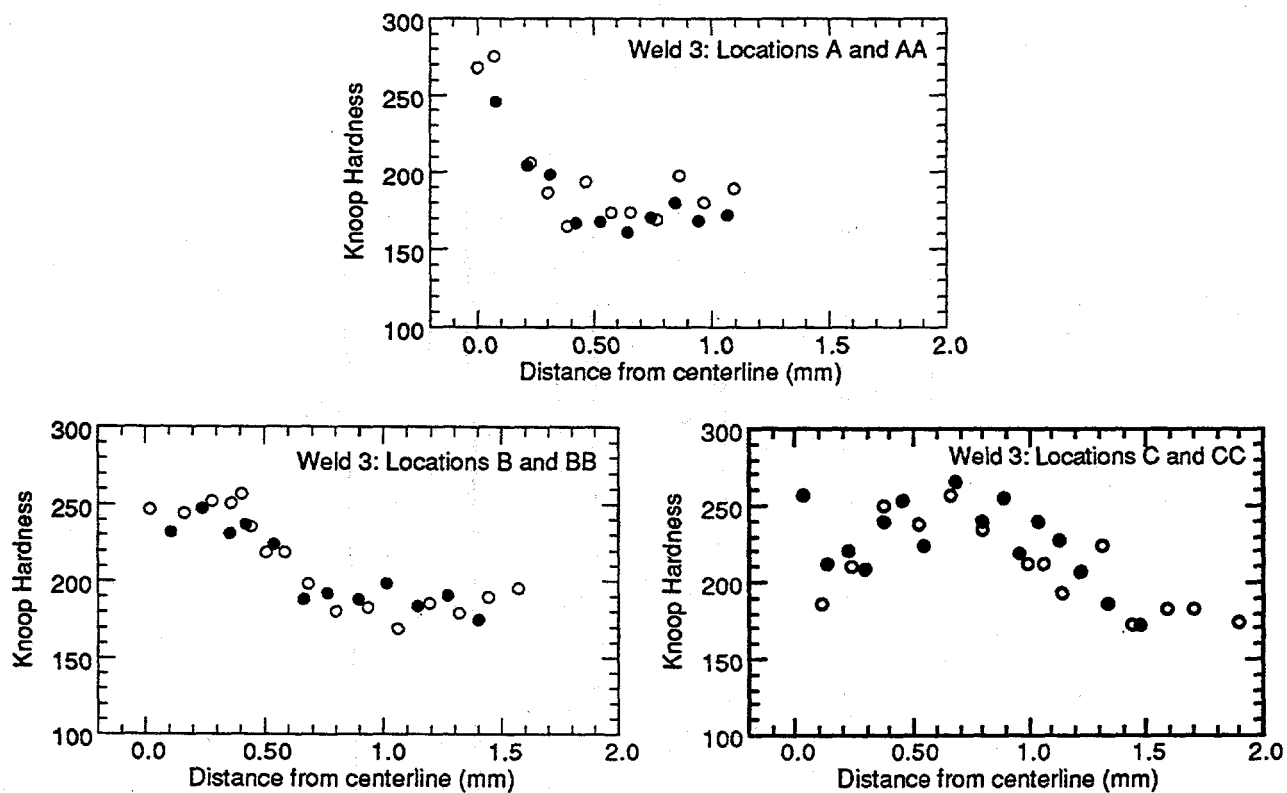
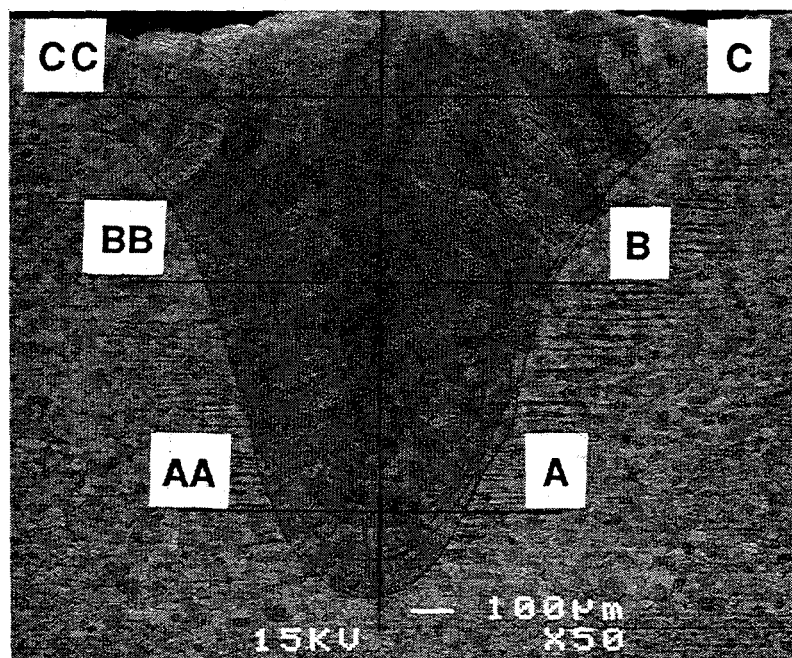


Figure 1. Hardness profiles at elevations indicated in photomicrograph for laser-welded V-4Cr-4Ti specimen in as-welded condition, designated as Weld 3 in Table 1. Open and closed symbols represent hardness values measured on either side of weld centerline.

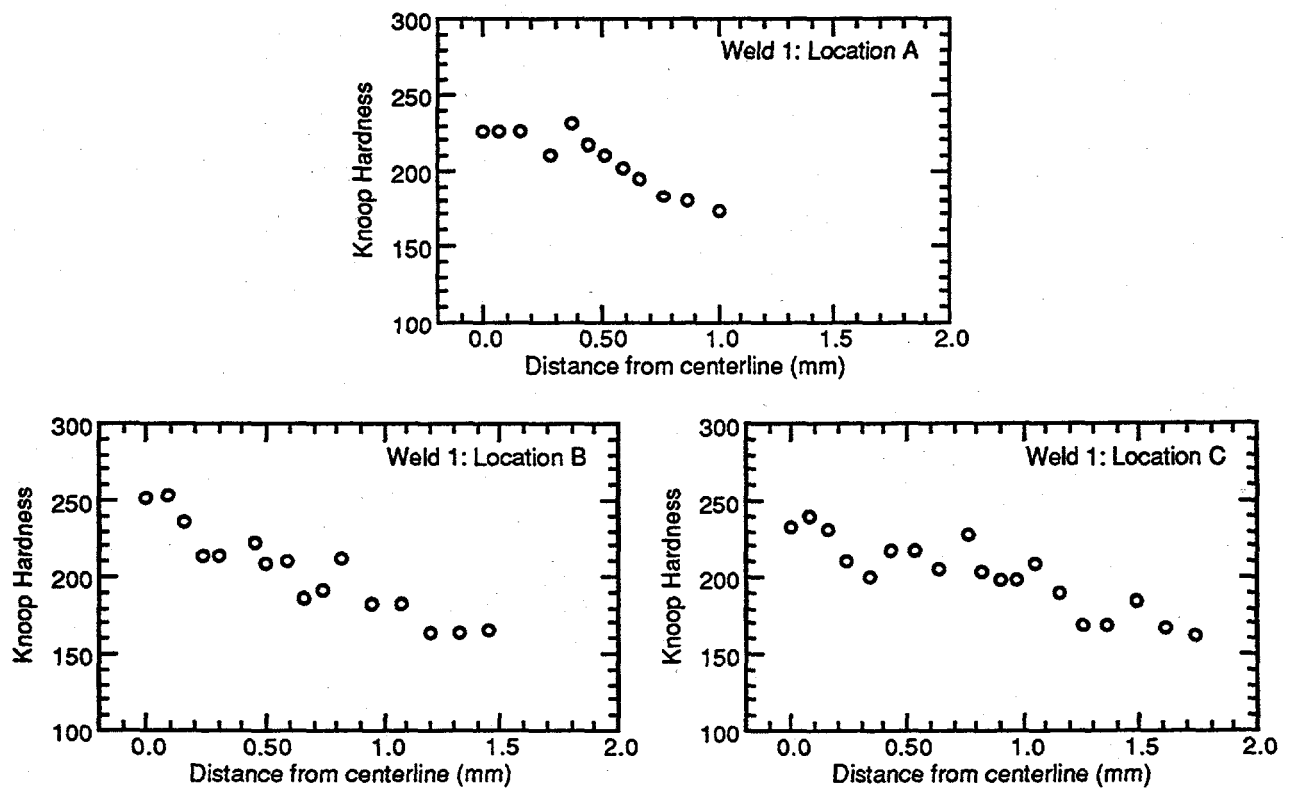
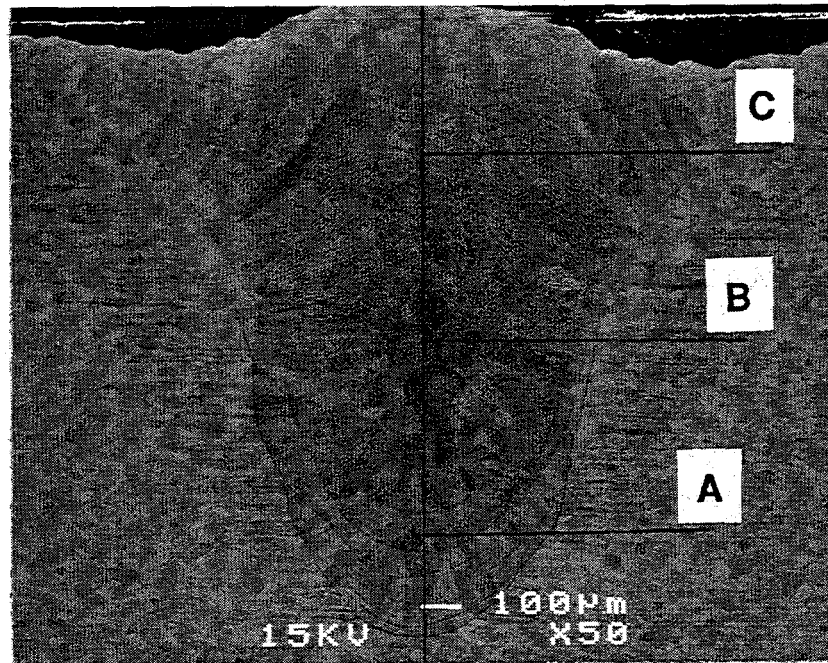


Figure 2. Hardness profiles at several elevations indicated in photomicrograph for laser-welded V-4Cr-4Ti specimen after post-welding treatment, designated as Weld 1 in Table 1.

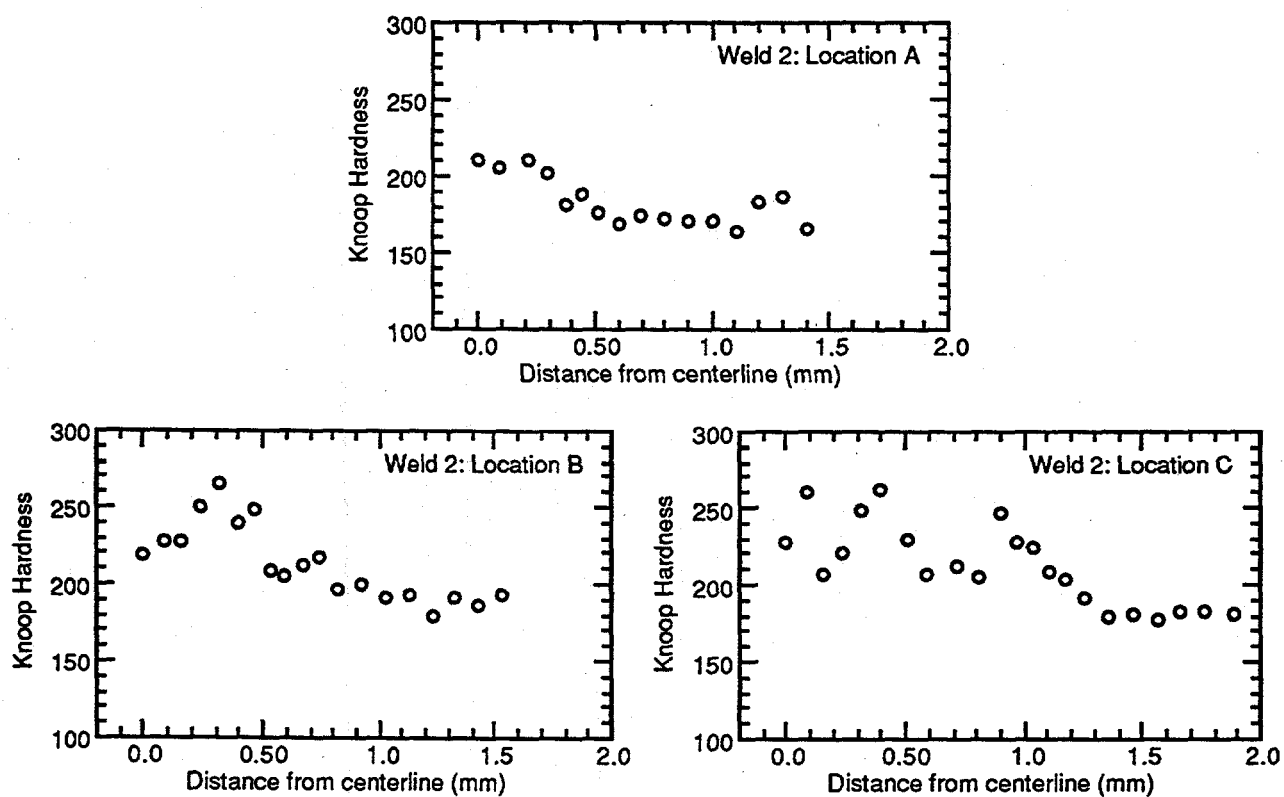
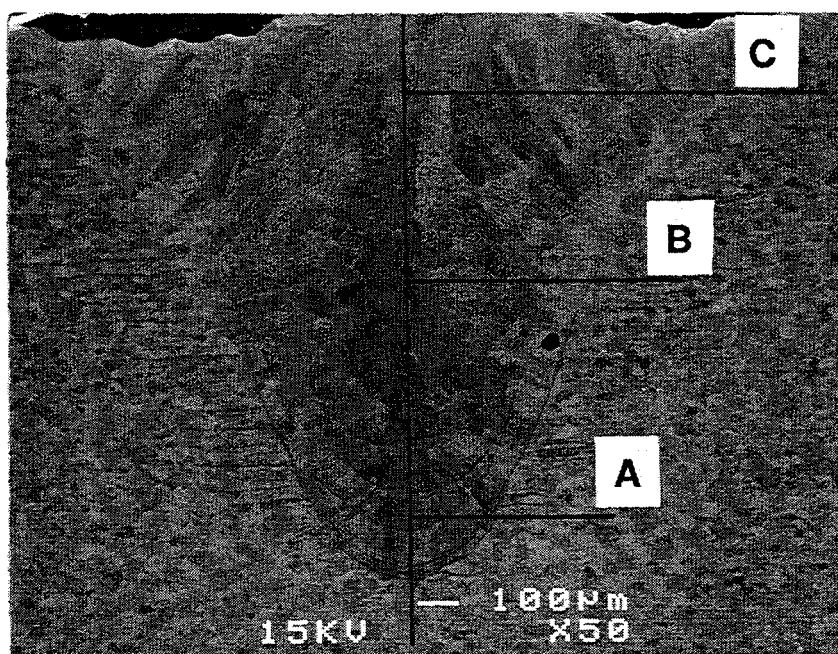


Figure 3. Hardness profiles at several elevations indicated in photomicrograph for laser-welded V-4Cr-4Ti specimen after post-welding treatment, designated as Weld 2 in Table 1.